Late Gadolinium Enhanced Cardiac Magnetic Resonance Imaging Radiomics For High Precision Differentiation of Scar and Viable Cardiac Tissues

Elham Avard, Isaac Shiri, Ghasem Hajianfar, Hamid Abdollahi, Kian Kasani, Kiara Rezaei kalantari, Ahmad Bitarafan-rajabi, Mohammad Reza Deevband, Mehrdad Oveisi, and Habib Zaidi, *Fellow, IEEE*

2020 IEEE Nuclear Science Symposium and Medical Imaging Conference (NSS/MIC) | 978-1-7281-7693-2/20/$31.00 ©2020 IEEE | DOI: 10.1109/NSS/MIC42677.2020.9507746

***Abstract*– The aim of this work is to determine the radiomic features and develop a machine learning algorithm for high precision differentiation between scar and viable tissues in the left ventricular myocardium on Late Gadolinium Enhanced Cardiac Magnetic Resonance (LGE-CMR) images. This work involves patients referred for post-myocardial infarction (MI) with scar tissue in their left ventricles. Forty-two patients were included in the current study. All images were segmented and verified simultaneously by two radiologists using 3D-Slicer software. Radiomic features including intensity-based, texture-based and shape-based features were extracted from different regions. Hierarchical clustering was performed for unsupervised grouping of scar and viable tissues that differentiate them with one error in normal tissue. Multiple support vector machine recursive feature elimination (MSVM-RFE) was used for feature selection. For classification purposes, Support Vector Machine (SVM) and Random Forest (RF) were used in this study. Linear SVM with AUC of 0.99 ± 0.02, sensitivity of 0.99 ± 0.02 and specificity of 0.99 ± 0.02 yielded the best results. This work demonstrated that using radiomics on LGE-CMR images could accurately detect the scar tissue, which could potentially incorporate automated segmentation and classification tools in LGE-CMR.**

***Index Terms*— MRI, gadolinium enhancement, radiomics, machine learning, myocardial infarction**

Manuscript was submitted Dec 20, 2020. This work was supported by Shahid Beheshti University of Medical Sciences under grant number IR.SBMU.MSP.REC.1398.811 and the Swiss National Science Foundation under grant SNSF 320030_176052.

E. Avard and M.R Deevband are with Department of Biomedical Engineering and Medical Physics, Shahid Beheshti University of medical sciences, Iran (e-mail: elham.avard@gmail.com, mdeevband@sbmu.ac.ir).

I. Shiri and H. Zaidi are with Division of Nuclear Medicine and Molecular Imaging, Geneva University Hospital, CH-1211 Geneva, Switzerland (e-mail: Isaac.shirilord@unige.ch, habib.Zaidi@hcuge.ch).

G. Hajianfar, K. Kasani, K.R kalantari, A. Bitarafan-rajabi and M. Oveisi are with Rajaie Cardiovascular Medical and Research Center, Iran University of Medical Science, Tehran, Iran (e-mail: hajianfar.gh@gmail.com, kian.kasani@yahoo.com, rkkiara@gmail.com, bitarafan@hotmail.com, moveisi@cs.ubc.ca).

Hamid Abdollahi is with Department of Radiologic Sciences and Medical Physics, Kerman University of Medical Science, Kerman, Iran (e-mail: hamid_rbp@yahoo.com).

Mehrdad Oveisi is with University of British Colombia (e-mail: moveisi@cs.ubc.ca).

Habib Zaidi is with Geneva University Neurocenter, Geneva University, Geneva, Switzerland (e-mail: habib.Zaidi@hcuge.ch).

I. Introduction

Cardiovascular diseases (CVDs) are the main leading causes of death worldwide. In some CVDs, such as myocardial infarction, ventricular myocardium partially loses its functionality [1]. This is named scar. It was shown that Late Gadolinium Enhancement Cardiac Magnetic Resonance (LGE-CMR) imaging is a feasible approach to examine the viability of left ventricular myocardium muscles [2]. Detecting the precise location and size of infarction are important prognostic factors for precision medicine, including implanting Implantable Cardioverter-Defibrillators (ICDs) in patients [3].

Recently, radiomics emerged as a new approach for better detection, diagnosis, prediction and prognostication [4-12]. Radiomics analysis was investigated in the context of CVD studies, demonstrating that radiomics could diagnose and identify high and low risk of post-myocardial infarction arrhythmia [13], cardiac risk prediction [14], differentiation between acute, subacute and chronic myocardial infarction [2, 15], myocardial infarction and myocarditis [16], and scar and healthy myocardium tissue [17].

Any robust differentiation between scar and normal tissue is important for high accuracy diagnosis and precision medicine [18]. In the current study, LGE-CMR images were used to find radiomic features and develop machine learning algorithm for high precision differentiation of scar and viable tissues in the left ventricular myocardium. Currently, manual and semi-manual methods are used for scar detection.

II. Materials and Methods

Radiomics analysis included different steps as elaborated in the following sections.

A. Study population

This work included patients referred for post-myocardial infarction with scar tissue in their left ventricles. Those experiencing myocarditis and cases that did not have any scars diagnosed in their left ventricle were excluded from this study. After applying inclusion and exclusion criteria, 42 patients including 6 women (mean ±SD age of 63.5± 13.4) and 36 men (mean ±SD age of 58.5 ± 11.9 years) were studied.

978-1-7281-7693-2/20/$31.00 ©2020 IEEE

B. MR image acquisition

MR imaging was performed using a 1.5 Tesla MRI scanner. LGE-CMR images were obtained approximately 10 minutes after bolus injection of 0.15 mmol/kg Gd-DTPA. A 2D Phase-Sensitive Inversion-Recovery (PSIR) sequence was used (TR 683 ms, TE 1.23 ms, flip angle 45°, FOV 340 × 340 mm^2, and resolution 1.8 × 1.8 × 8 mm^3). The slice thickness was 8 mm, with 8 mm slice interval. The images were taken at MRI PSIR in short-axis view.

C. Region of interest definition

All images were segmented and verified simultaneously by two radiologists (with 5 and 7 years of experience in cardiovascular imaging) using the 3D-Slicer software [12]. The left ventricular myocardium was selected as a total region of interest. This was then divided into two parts corresponding to scar and normal tissue.

D. Pre-processing and feature extraction

In the pre-processing step, all images were resized to isotropic voxel size. Then, radiomic features were extracted through the PyRadiomics open source python library [13]. These features include intensity-based, texture-based and shape-based features. One hundred and seven features were extracted.

E. Unsupervised clustering

Hierarchical clustering was performed for unsupervised grouping of scar and viable tissues. In hierarchical clustering, each cluster is distinct from each other (scar and viable), and the objects within each cluster are broadly similar to each other.

F. Feature Selection and Classification

Multiple support vector machine recursive feature elimination (MSVM-RFE) was used for feature selection [14]. The CARET package [15] from R software is used for implementing Linear and Radial algorithms for SVM classifier and Ranger and RF algorithms for RF classifier. For all algorithms, we first trained the machine with the top five features and then the ranked features returned by the MSVM-RFE were progressively added one by one, from most to least important. Each feature subset is then used to train multivariate algorithms.

G. Evaluation

The area under the curve (AUC) of receiver operating characteristic (ROC), diagnostic sensitivity and specificity were reported, whereas a 10-fold cross validation was used for multivariate models.

III. RESULT

Fig. 1 presents the hierarchical clustering of scar and viable tissues. The clustering performed very well in discriminating these tissues with one error in normal tissues.

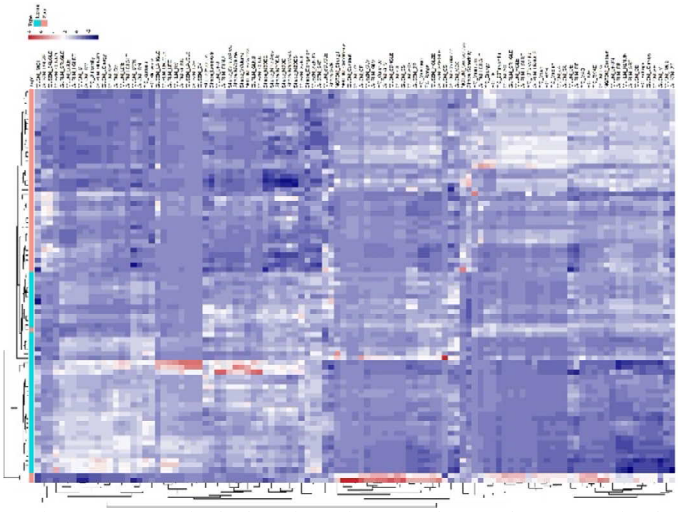

Fig. 1. Unsupervised clustering of scar and normal segments in the datasets.

Fig. 2 shows an example of radiomics feature map with high AUC in differentiating scar and normal cardiac tissues in different cases. Different feature maps present different characteristics of scare regions. Fig. 3 depicts a representative example of radiomics feature map, which failed to differentiate scar and normal cardiac tissues.

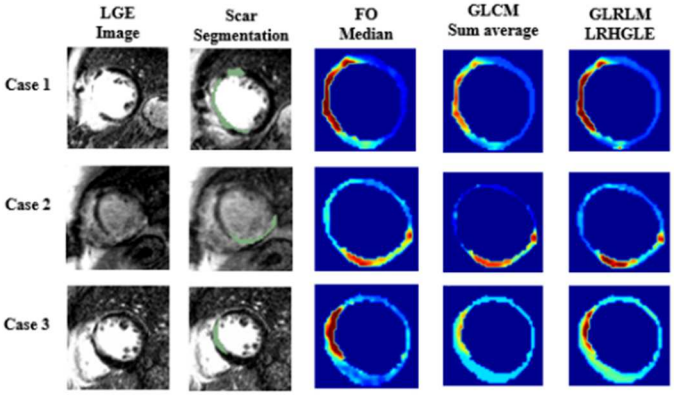

Fig. 2. Example of radiomics feature with high AUC in differentiation of scar and normal cardiac tissues map in different cases.

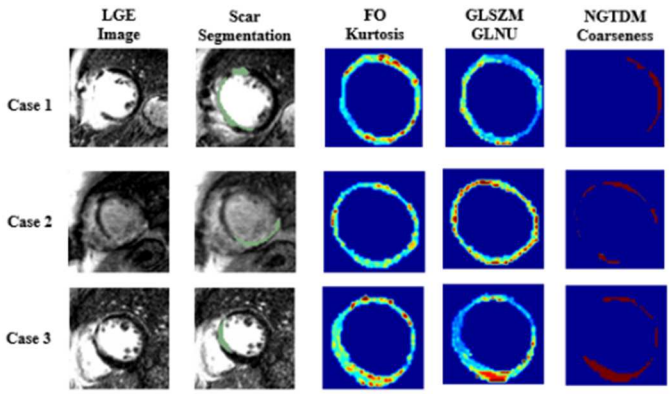

Fig. 3. Example of radiomics feature with low AUC in differentiation of scar and normal cardiac tissues map in different cases.

The top 10 features obtained by SVM algorithm are include three intensity-based features (median, skewness and mean), one shape-based feature (sphericity) and six texture-based

features (joint average, sum average and autocorrelation from GLCM, size zone non-uniformity and small area high gray level emphasis related to GLSZM and long run high gray level emphasis from GLRLM). Table I summarizes the AUC for different classifiers. Linear SVM with AUC = 0.99 ± 0.02, sensitivity = 0.99 ± 0.02 and specificity = 0.99 ± 0.02 yielded the best results.

TABLE I. AUC sensitivity, specificity values and the least number of features that yields the best results for each algorithm.

Method	AUC	Sensitivity	Specificity	Number of Features
RF	0.95±0.02	0.99±0.02	0.92±0.03	**8**
SVM Linear	0.99±0.02	0.99±0.02	0.99±0.02	**12**
SVM Radial	0.94±0.03	0.96±0.05	0.91±0.00	**12**

Fig. 4 presents the AUC, sensitivity and specificity of machine learning algorithms. Ranger, RF and radial SVM methods had AUC of 0.95±0.01, 0.95±0.02 and 0.94±0.03 respectively.

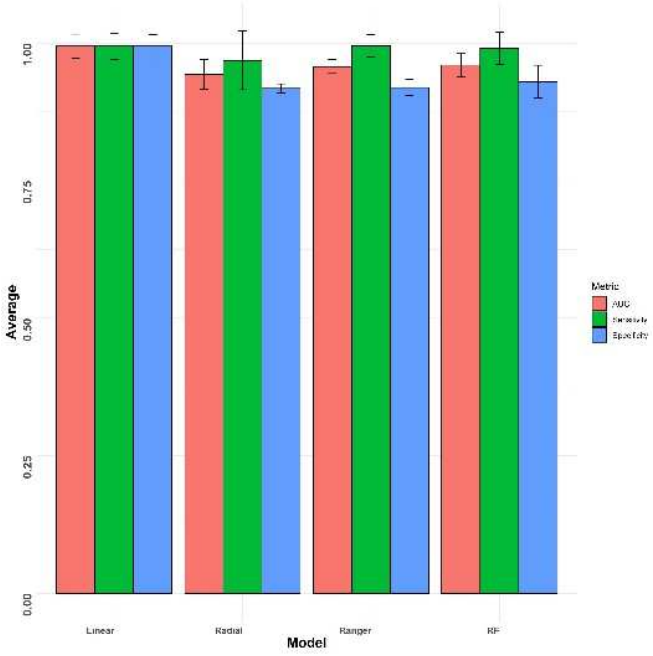

Fig. 4. Comparison of average AUC, sensitivity and specificity of various multivariate methods.

IV. Discussion

Accurate description of scar characteristics (size and location) is essential to assess the viability of the ventricular myocardium [16]. In this work, we analyzed the feasibility of radiomic features extracted from LGE-CMR images by SVM and RF supervised algorithms to distinguish between normal and scar tissues in the myocardium. Some radiomic features showed high performance in differentiating between scar and healthy tissues. We found that linear SVM (AUC = 0.99 ± 0.02, sensitivity = 0.99 ± 0.02 and specificity = 0.99 ± 0.02) yielded optimal results as the best machine learning algorithm for this radiomics analysis.

This work was performed on LGE-CMR for classification of scar tissues in contrast to previous studies that focused on non-enhanced images. In the current study, we aimed to find out the highly capable radiomic features and machine learning algorithm for discriminating scar tissue from LGE-CMR. Clinical routine segmentation algorithms mostly rely on intensity of images. However, we determined the radiomics feature which accurately detects scar tissue (the performance of these features was improved by machine learning algorithms). In our work, the range of AUC was 0.94-0.99, where an AUC of 0.99 was achieved by linear SVM and 0.94 by non-linear SVM, respectively. In addition, the methodology followed in this work could be combined with an automated segmentation algorithm, which divides the cardiac myocardium into different segments to classify each segment apart for detecting the scar tissue in the myocardium. Machine and deep learning-based algorithms emerged as a promising approach for accurate segmentation of the myocardium [19].

In this work, CMR images were manually segmented without using pathological information of scars, which might impact the definition of scar tissue. However, our algorithm performed very well in term of quantitative analysis with respect to manual segmentation. The small sample size with no external validation dataset would be another limitation of the current study. Repeatability and reproducibility of proposed radiomics features should be investigated to provide a generalizable model [20, 21]. Future work will assess the proposed model using a larger size of the external validation set.

V. Conclusion

The median from FO, LDLGLE from GLDM and IFMN from GLCM showed the highest performance in differentiating scar and viable tissues. Linear SVM yielded optimal results as the best machine learning algorithm for this radiomics analysis study. This work has shown that using radiomics on LGE-CMR images is able to accurately detect the scar tissue, and as such, could potentially be used as automated segmentation and classification tool in LGE-CMR imaging.

References

[1] M. Bayeva, K. T. Sawicki, J. Butler, M. Gheorghiade, and H. Ardehali, "Molecular and cellular basis of viable dysfunctional myocardium," (in eng), *Circ Heart Fail,* vol. 7, no. 4, pp. 680-691, 2014, doi: 10.1161/CIRCHEARTFAILURE.113.000912.

[2] B. Baessler, M. Mannil, S. Oebel, D. Maintz, H. Alkadhi, and R. Manka, "Subacute and Chronic Left Ventricular Myocardial Scar: Accuracy of Texture Analysis on Nonenhanced Cine MR Images," (in eng), *Radiology,* vol. 286, no. 1, pp. 103-112, Jan 2018, doi: 10.1148/radiol.2017170213.

[3] K. H. Schuleri *et al.*, "Cardiovascular magnetic resonance characterization of peri-infarct zone remodeling following myocardial infarction," *Journal of Cardiovascular Magnetic Resonance,* vol. 14, no. 1, p. 24, 2012.

[4] S. Mostafaei *et al.*, "CT imaging markers to improve radiation toxicity prediction in prostate cancer radiotherapy by stacking regression algorithm," *La radiologia medica,* vol. 125, no. 1, pp. 87-97, 2020.

[5] M. Nazari, I. Shiri, and H. Zaidi, "Radiomics-based machine learning model to predict risk of death within 5-years in clear cell renal cell carcinoma patients," (in eng), *Comput Biol Med,* vol. 129, p. 104135, Nov 23 2020, doi: 10.1016/j.compbiomed.2020.104135.

[6] S. Rastegar *et al.*, "Radiomics for classification of bone mineral loss: A machine learning study," (in eng), *Diagn Interv Imaging,* vol. 101, no. 9, pp. 599-610, Sep 2020, doi: 10.1016/j.diii.2020.01.008.

[7] M. Nazari *et al.*, "Noninvasive Fuhrman grading of clear cell renal cell carcinoma using computed tomography radiomic features and machine learning," (in eng), *Radiol Med,* vol. 125, no. 8, pp. 754-762, Aug 2020, doi: 10.1007/s11547-020-01169-z.

[8] G. Hajianfar *et al.*, "Noninvasive O6 Methylguanine-DNA Methyltransferase Status Prediction in Glioblastoma Multiforme Cancer Using Magnetic Resonance Imaging Radiomics Features: Univariate and Multivariate Radiogenomics Analysis," *World Neurosurgery,* vol. 132, pp. e140-e161, 2019/12/01/ 2019, doi: https://doi.org/10.1016/j.wneu.2019.08.232.

[9] H. Arabi, A. AkhavanAllaf, A. Sanaat, I. Shiri, and H. Zaidi, "The promise of artificial intelligence and deep learning in PET and SPECT imaging," (in eng), *Phys Med,* vol. 83, pp. 122-137, Mar 22 2021, doi: 10.1016/j.ejmp.2021.03.008.

[10] I. Shiri *et al.*, "Machine learning-based prognostic modeling using clinical data and quantitative radiomic features from chest CT images in COVID-19 patients," (in eng), *Comput Biol Med,* vol. 132, p. 104304, May 2021, doi: 10.1016/j.compbiomed.2021.104304.

[11] H. Abdollahi, I. Shiri, and M. Heydari, "Medical Imaging Technologists in Radiomics Era: An Alice in Wonderland Problem," (in eng), *Iran J Public Health,* vol. 48, no. 1, pp. 184-186, Jan 2019.

[12] S. P. Shayesteh *et al.*, "Treatment Response Prediction using MRI-based Pre-, Post- and Delta-Radiomic Features and Machine Learning Algorithms in Colorectal Cancer," (in eng), *Med Phys,* Apr 24 2021, doi: 10.1002/mp.14896.

[13] L. P. Kotu, K. Engan, T. Eftestøl, L. Woie, S. Ørn, and A. K. Katsaggelos, "Local Binary Patterns used on Cardiac MRI to classify high and low risk patient groups," in *2012 Proceedings of the 20th European Signal Processing Conference (EUSIPCO)*, 27-31 Aug. 2012 2012, pp. 2586-2590.

[14] E. K. Oikonomou *et al.*, "A novel machine learning-derived radiotranscriptomic signature of perivascular fat improves cardiac risk prediction using coronary CT angiography," *European Heart Journal,* vol. 40, no. 43, pp. 3529-3543, 2019, doi: 10.1093/eurheartj/ehz592.

[15] A. Larroza, A. Materka, M. P. Lopez-Lereu, J. V. Monmeneu, V. Bodi, and D. Moratal, "Differentiation between acute and chronic myocardial infarction by means of texture analysis of late gadolinium enhancement and cine cardiac magnetic resonance imaging," (in eng), *European journal of radiology,* vol. 92, pp. 78-83, Jul 2017, doi: 10.1016/j.ejrad.2017.04.024.

[16] T. Di Noto *et al.*, "Radiomics for Distinguishing Myocardial Infarction from Myocarditis at Late Gadolinium Enhancement at MRI: Comparison with Subjective Visual Analysis," *Radiology: Cardiothoracic Imaging,* vol. 1, no. 5, p. e180026, 2019/12/01 2019, doi: 10.1148/ryct.2019180026.

[17] A. Larroza, M. Lopez-Lereu, J. Monmeneu, V. Bodi, and D. Moratal, *Texture analysis for infarcted myocardium detection on delayed enhancement MRI*. 2017, pp. 1066-1069.

[18] K. C. Lee, J. Dretzke, L. Grover, A. Logan, and N. Moiemen, "A systematic review of objective burn scar measurements," *Burns & Trauma,* vol. 4, no. 1, p. 14, 2016/04/27 2016, doi: 10.1186/s41038-016-0036-x.

[19] S. Moradi *et al.*, "MFP-Unet: A novel deep learning based approach for left ventricle segmentation in echocardiography," *Physica Medica,* vol. 67, pp. 58-69, 2019/11/01/ 2019, doi: https://doi.org/10.1016/j.ejmp.2019.10.001.

[20] M. Edalat-Javid *et al.*, "Cardiac SPECT radiomic features repeatability and reproducibility: A multi-scanner phantom study," (in eng), *J Nucl Cardiol,* Apr 24 2020, doi: 10.1007/s12350-020-02109-0.

[21] I. Shiri *et al.*, "Repeatability of radiomic features in magnetic resonance imaging of glioblastoma: Test-retest and image registration analyses," (in eng), *Med Phys,* vol. 47, no. 9, pp. 4265-4280, Sep 2020, doi: 10.1002/mp.14368.